

Impact of Heterogeneous Fading Channels in Power Limited Cognitive Radio Networks

Shaojie Zhang¹, Abdelhakim Senhaji Hafid, *Member, IEEE*, Haitao Zhao, *Member, IEEE*,
and Shan Wang, *Member, IEEE*

Abstract—The tradeoff between decreasing the interference to primary user (PU) and increasing secondary users' (SUs') achievable throughput is an important problem in cognitive radio networks. Heterogeneous fading channels from PU to multiple SUs, PU's traffic distribution, limited SU's power and multiple SUs' access contention impact both these two conflicting objectives. In this paper, we study the joint impact of these four factors on the tradeoff. More specifically, we consider that the channels from PU to SUs are exposed to non-identically independent free space path losses, PU's traffic randomly arrives and departs from the channel, every SU's average power consumption is limited, while multiple SUs contend to transmit. We first model the impact of these factors on SUs' spectrum sensing and data transmission. Then, we formulate the tradeoff aiming at maximizing SUs' aggregated throughput under two constraints: 1) interference probability to PU and 2) SUs' average power consumption. To solve the optimization problem, we design a novel cluster based particle swarm optimization (C-PSO) algorithm. By iteratively updating the particles in a cluster based on the comparison of their fitnesses, the cluster converges to the optimal solution rapidly. Simulation results validate the feasibility of the C-PSO algorithm and the outperformance of our proposal compared against related contributions which consider the homogeneous fading channel. They also show how the optimal solution varies with path losses and PU's traffic distribution.

Index Terms—Cognitive radio networks, heterogeneous fading channels, cluster based particle swarm optimization.

I. INTRODUCTION

OPPORTUNISTIC spectrum access (OSA) based cognitive radio networks (CRNs) enable secondary users (SUs) to opportunistically use the spectrum when detecting the absence of primary user (PU) [1], [2]. It is a promising technology to solve the problem of under-utilization and the rapidly increasing demand of spectrum resources. It provides

Manuscript received May 1, 2017; revised September 11, 2017 and November 20, 2017; accepted November 28, 2017. Date of publication December 4, 2017; date of current version March 7, 2018. This work was supported in part by National Natural Science Foundation of China No. 61471376, 61401492, and 61601480. The associate editor coordinating the review of this paper and approving it for publication was A. B. MacKenzie. (*Corresponding author: Haitao Zhao.*)

S. Zhang is with the Army Aviation Institute and the Academy of Military Sciences of PLA, Beijing 101149, China (e-mail: zhangshaojie@nudt.edu.cn).

A. S. Hafid is with the Department of Computer Science and Operations Research, University of Montreal, Montreal, QC H3C 3J7, Canada (e-mail: ahafid@iro.umontreal.ca).

H. Zhao and S. Wang are with the College of Electronic Science, National University of Defense Technology, Changsha 410073, China (e-mail: haitaozhao@nudt.edu.cn; chinafir@nudt.edu.cn).

Digital Object Identifier 10.1109/TCCN.2017.2779858

potential spectrum resources for 5G and other future networks [3], [4]. For SUs, in order to discover and reuse the idle spectrum, a periodical frame structure, consisting of a sensing duration followed by a transmission duration, is widely used. Previous contributions [5], [6] have shown that a longer sensing duration improves the sensing reliability and thus causes less interference to PU. However, with fixed frame duration, the longer sensing duration also decreases the time left for SUs' data transmission and may degrade SUs' throughput. Therefore, decreasing the interference to PU and increasing SUs' throughput are two conflicting objectives in CRNs, and understanding the tradeoff between them is fundamental to optimize the performance of OSA based CRNs.

Liang *et al.* [6] first formulated this tradeoff mathematically considering the imperfect spectrum sensing and proved the existence of the optimal sensing duration which maximizes secondary throughput with a targeted detection probability. Zhang *et al.* [7] and Zhang and Yeo [8] extended this research to study respectively the impact of energy consumption and the cooperative spectrum sensing on this tradeoff. The PU's traffic in these contributions was assumed to be either present or absent throughout the entire frame duration, which ignores the random departure and arrival of PU's traffic in realistic CRNs. Therefore, Tang *et al.* [9] modeled the realistic PU's traffic and analyzed the impact of PU's traffic on this tradeoff. All these contributions considered the tradeoff only from the PHY perspective, in the presence of imperfect spectrum sensing. However, they ignored the impact of multiple SUs' access contention in MAC. In [10]–[12], we studied the tradeoff from a cross-layer (PHY and MAC) perspective and modeled multiple SUs' access contention to maximize SUs' aggregated throughput while restricting the interference probability to PU under a predefined threshold.

One common assumption used in our previous researches [10]–[12] is that wireless channels from PU to all SUs are homogeneous. More specifically, the conditions of the channels from PU to all SUs are the same so that PU's signal received by all SUs is the same. This assumption forces all SUs to produce the same spectrum sensing result and thus to make the same determination of spectrum access. Unfortunately, in reality, wireless channels from PU to multiple SUs vary dramatically, for instance, due to the different distances from PU to SUs. The heterogeneous fading channels cause that PU's signal-to-noise ratios (SNRs) received by different SUs are not the same. Thus, SUs make different sensing results, according to which each

SU individually determines to access the channel or not. Additionally, SUs in most CRNs are power limited and they spend some power for spectrum sensing and use the remaining power for data transmission. Thus, considering heterogeneous fading channels and power efficiency, SUs need to adapt their transmission rates based on the received PU's SNR and the remaining data transmission power. To conclude, the heterogeneous fading channels do have an impact on both the interference probability to PU and SUs' throughput performance in power limited CRNs. The impact of heterogeneous sensing and reporting channel qualities and energy efficiency has been studied in [13] and [14]. However, to the best of our knowledge, there is no existing contribution taking into account all these four practical characteristics: (1) heterogeneous fading channels from PU to SUs, (2) power limited SUs, (3) random arrival and departure of PU's traffic within SUs' frame, and (4) multiple SUs' access contention.

To fill this blank, we consider the joint impact of the above four characteristics and then study the tradeoff between the interference probability to PU, SUs' throughput and SUs' power consumption. The main contributions of this paper are twofold.

- *New Problem:* The considered CRN has the following characteristics: (1) heterogeneous fading channels from PU to SUs, (2) power limited SUs, (3) random arrival and departure of PU's traffic within SUs' frame, and (4) multiple SUs' access contention. Although these four characteristics have been studied in our prior work [10]–[12] and related contributions [13], [14] respectively, problem formulation considering all these four characteristics has not been studied yet. We derive the closed-form expressions of the interference probability to PU, SUs' aggregated throughput and SUs' average power consumption, jointly considering the above four characteristics. Then, we formulate the tradeoff problem aiming at maximizing SUs' throughput satisfying interference probability and average power consumption constraints.
- *New Solution:* We analyze the convexity of the problem and propose a cluster based particle swarm optimization (C-PSO) algorithm. By iteratively updating the particles in a cluster based on the comparison of their fitnesses, the cluster converges to the optimal solution rapidly. The optimal solution, including the optimal sensing duration, frame duration, detection threshold and transmission power, for the tradeoff problem is obtained. Simulation results show that C-PSO algorithm can solve the optimization problem with lower computational complexity. Meanwhile, by considering heterogeneous fading channels, our proposal achieves better throughput performance compared to related contributions which assume the same fading channels. This is the first research to apply C-PSO algorithm in the optimization of CRNs.

The rest of the paper is organized as follows. Section II introduces related work. Section III describes the system model and presents the cross-layer formulation of the tradeoff problem. In Section IV, we describe C-PSO algorithm. Section V presents simulation results and compares the

performance with related contributions. Finally, Section VI concludes the paper.

II. RELATED WORK

Since the tradeoff between increasing SUs' throughput and decreasing the interference to PU is imperative in cognitive radio systems, there are abundant contributions on this topic, aiming at computing the optimal sensing parameters. Based on different factors that impact the tradeoff problem, these contributions can be classified into four categories.

The first category studied more practical PU's traffic distribution. Tang *et al.* [9] first modeled the practical PU's traffic distribution as an alternating renewable process and studied the impact of PU's random arrival and departure on the detection probability and false alarm probability. Random arrivals and departures of one single PU and multiple PUs within SU's frame were studied in [15] and [16] respectively. Xing *et al.* [17] studied PU's access pattern and modeled PU's presence and absence within several successive frames. Chen and Oh [18] investigated various spectrum occupancy models from measurement campaigns taken around the world. These contributions proved that, considering more practical PU's traffic distribution, both sensing duration and frame duration impact the tradeoff and thus should be jointly optimized.

The second category studied SU's access contention. In [10], we proposed a cross-layer analytical model, which quantifies the impact of imperfect spectrum sensing in PHY and access contention in MAC on SU's transmission probability. Two widely-used MAC protocols were considered as examples to validate the feasibility of the proposed model. Based on this contribution [10], the impacts of multiple channels access and the cooperative sensing were respectively studied in [11] and [12]. In [19], the throughput model involving channel handoff and collisions with PU was proposed. By balancing the misdetection and false alarm probabilities and maximizing the SU's throughput subject to the sensing quality and collision avoidance constraints, the optimal frame structure was computed.

The third category studied the heterogeneous fading channels. Celik *et al.* [20] studied heterogeneous SNRs and imperfect common control channel (CCC) in energy harvesting cooperative spectrum sensing (CSS). The achievable throughput was maximized by optimizing the asymptotic active probability, sensing duration, and detection threshold of each SU. They also considered heterogeneous CRNs comprising multiple primary channels (PCs) with heterogeneous characteristics and SUs with various sensing and reporting qualities for different PCs [21]. The subset of PCs, SU assignment for each chosen PC, sensing duration and detection threshold were jointly optimized with the objective of minimizing the unit energy spent per transmitted bit. To overcome the poor sensing quality caused by heterogeneous fading channels, various cooperative spectrum sensing schemes were designed [22]–[24].

The fourth category studied the energy efficiency issue. Ng *et al.* [14] studied multiple-input single-output (MISO) secondary communication systems with multi-antenna transmitter

and energy harvesting SUs. The throughput improvement resulting from the multi-antenna transmitter and the impact of the energy causality restraint were analyzed. Moghimi *et al.* [25] investigated the impact of transmit power on a multi-input multi-output (MIMO) cognitive radio system. They proposed a stochastic, energy-aware model and derived the optimal spectrum sensing interval to achieve the balance between energy consumption and SU's throughput. Yin *et al.* [26] proposed to use both data-based and decision-based fusion rules in energy harvesting cognitive radio systems. Liu *et al.* [27] and Hu *et al.* [28] investigated the energy efficiency in cooperative sensing.

In above contributions, the practical characteristics of CRNs, including PU's traffic distribution, SU's access contention, heterogeneous fading channels and limited SU's power, were studied respectively. To the best of our knowledge, there is no existing contribution taking into account all these characteristics. This motivated us to analyze and solve the tradeoff factoring all these four important characteristics.

III. PROBLEM FORMULATION

Consider a distributed CRN consisting of K SUs within a single-hop area as shown in Fig. 1(a). Each SU is equipped with only one antenna. The overlay spectrum sharing mechanism is used, and thus SUs communicate with each other only if the absence of PU's traffic is detected. In order to effectively discover and reuse the idle spectrum while avoiding harmful interference to PU, each SU in overlay based CRNs uses periodical frame structure, which consists of a sensing period T_{se} followed by a data transmission period T_{tr} . The frame duration T equals $T_{se} + T_{tr}$. During sensing period, energy detection is performed. Indeed, the received signal from PU in the licensed channel is pre-filtered by a band-pass filter with bandwidth B and then squared and summed up over T_{se} . We set sampling interval T_s to $1/B$ according to band-pass sampling theorem and thus the total number of samples I is $B \cdot T_{se}$. In the following, we will present the practical CRNs model in terms of heterogeneous fading channels and power limited SUs.

A. Heterogeneous Fading Channels

In order to model practical CRNs, we consider both heterogeneous fading channels from PU to multiple SUs and a realistic PU's traffic distribution. The channels from PU to SUs are exposed to non-identically independent free space path losses and h_k in Fig. 1(a) represents the channel coefficient from PU to SU_k . We use a practical PU's traffic model [9], where PU's traffic randomly arrives at or departs from the channel within a frame duration as shown in Fig. 1(b). To simplify the analysis, we assume that the frame duration is an integral multiple of sampling interval T_s , i.e., $T = J \cdot T_s$. This assumption is reasonable since $T_s \ll T$. The channel status changes at most once at the edge of a sample during a frame. The probability of two or more status changes is much smaller than the probability of a single status change. Thus, two or more status changes seldom happen such that they can be ignored [9].

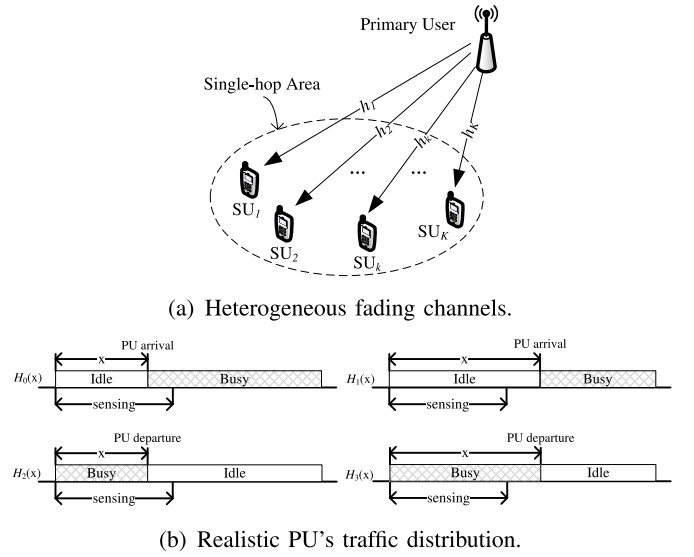


Fig. 1. System model with K SUs considering (a) heterogeneous fading channels, where h_k denotes the channel coefficient from PU to SU_k , and (b) realistic PU's traffic distribution, where x denotes the sample after which PU's traffic arrives at or departs from the channel.

Let s_i denote the PU's transmitted signal and n_i denote additive white Gaussian noise received at i th sample. Let h_k denote the channel coefficient from PU to SU_k . Energy detection result of SU_k , i.e., Y_k for $k \in \{1, 2, \dots, K\}$, can thus be written as the following quaternary hypothesis testing problem:

$$Y_k = \begin{cases} \sum_{i=1}^x (n_i)^2 + \sum_{i=x+1}^I (h_k \cdot s_i + n_i)^2, & 1 \leq x \leq I-1, H_0(x) \\ \sum_{i=1}^I (n_i)^2, & I \leq x \leq J, H_1(x) \\ \sum_{i=1}^x (h_k \cdot s_i + n_i)^2 + \sum_{i=x+1}^I (n_i)^2, & 1 \leq x \leq I-1, H_2(x) \\ \sum_{i=1}^I (h_k \cdot s_i + n_i)^2, & I \leq x \leq J, H_3(x) \end{cases} \quad (1)$$

where $H_0(x)$ (resp. $H_1(x)$) represents the arrival of PU's traffic after x th sample within sensing period (resp. data transmission period). $H_2(x)$ (resp. $H_3(x)$) represents the departure of PU's traffic after x th sample within sensing period (resp. data transmission period).

Considering the fact that energy detection is determined by SUs' received signal power, spectrum sensing is highly related to large-scale fading suffered by PU's signal. Therefore, to evaluate the impact of heterogeneous fading channels from PU to SUs, the representative free space path loss model with the additive white Gaussian noise [29] is used in this paper. If d_k and f denote the distance from PU to SU_k in kilometers (kms) and the working frequency in MHz respectively, path loss L_k in dB can be defined as follows

$$L_k = -32.4 - 20 \log_{10}(d_k) - 20 \log_{10}(f). \quad (2)$$

And channel gain $|h_k|^2$ can be expressed as $|h_k|^2 = 10^{L_k/10}$. Thus, PU's SNR received by SU_k when PU's traffic is present

can be derived as

$$\gamma_k = |h_k|^2 \cdot \gamma_p = \frac{10^{L_k/10} \cdot P_{pu}}{N_0}, \quad (3)$$

where γ_p represents PU's transmission SNR, P_{pu} represents PU's transmission power, i.e., $P_{pu} = \mathbb{E}(|s_i|^2)$, and N_0 represents the variance of additive white Gaussian noise, i.e., $N_0 = \mathbb{E}(|n_i|^2)$. Here, $\mathbb{E}(\cdot)$ represents expectation operator.

Considering the status transitions of the channel, the average SNR observed by SU_k is decided by the ratio of busy status duration to the whole sensing duration. In the above hypotheses, the average SNR of SU_k can be computed as $\gamma_{H_0(x)}^k = \frac{(I-x)\gamma_k}{I}$, $\gamma_{H_1(x)}^k = 0$, $\gamma_{H_2(x)}^k = \frac{x\gamma_k}{I}$ and $\gamma_{H_3(x)}^k = \gamma_k$ respectively. In CRNs, all SUs use common sensing duration I and detection threshold ε for spectrum sensing. The detection probability that SU_k detects the channel as busy in hypothesis $H_i(x)$, $i \in \{0, 1, 2, 3\}$, can be expressed as [6]

$$P_{B,H_i(x)}^k(I, \varepsilon) = \frac{1}{2} Q \left(\frac{\varepsilon - I - I \cdot \gamma_{H_i(x)}^k}{2\sqrt{I + 2I \cdot \gamma_{H_i(x)}^k}} \right), \quad (4)$$

where $Q(\cdot)$ denotes the complementary error function of the standard Gaussian distribution, i.e., $Q(x) = \frac{1}{\sqrt{2\pi}} \int_x^\infty e^{-t^2/2} dt$. We observe that the heterogeneous fading channels enable SUs to produce different detection results (except hypothesis $H_1(x)$).

B. Power Limited SUs

After spectrum sensing, SUs which detect the channel as idle will opportunistically access the channel. For long-term statistics, SUs can be considered to transmit with a stable probability after detecting the channel as idle. This conditional transmission probability depends on MAC protocol, SUs' traffic load and the interference probability to PU [30], [31]. We define this conditional transmission probability as α , i.e., each SU transmits a packet with probability α under the condition that it has detected the channel as idle. Thus, SU_k 's transmission probability in hypothesis $H_i(x)$ can be expressed as

$$P_{tr,H_i(x)}^k = \left(1 - P_{B,H_i(x)}^k(I, \varepsilon)\right) \cdot \alpha. \quad (5)$$

Since SUs detect the channel as idle with different probabilities due to heterogeneous fading channels, SUs' transmission probabilities are also different.

According to Shannon's theory, SU_k 's achievable transmission rate in hypothesis $H_i(x)$ can be computed as

$$R_{H_i(x)}^k = B \cdot \log_2 \left(1 + \frac{P_{tr}^k}{(1 + \gamma_{H_i(x)}^k)N_0} \right), \quad (6)$$

where P_{tr}^k represents SU_k 's transmission power. If the data transmission is successful, the normalized throughput of SU_k within a frame can be expressed as

$$G_{H_i(x)}^k = \frac{J-I}{J} R_{H_i(x)}^k. \quad (7)$$

It is worth noting that in power limited CRNs, every SU's average power consumption for both sensing and transmission

cannot exceed a predefined threshold \bar{P} . Since SUs transmit with different transmission probabilities, the remaining transmission powers for different SUs are different despite using the same threshold \bar{P} . This allows SUs to obtain different transmission rates and different normalized throughputs within a successful frame.

C. Formulation of the Tradeoff Problem

In this section, we first model the channel status change and compute the probability of each hypothesis. Then, considering the joint impact of heterogeneous fading channels and power limited SUs, we derive the expressions of three key metrics, i.e., interference probability to PU, SUs' aggregated throughput and SUs' average power consumption.

Assuming that busy duration and idle duration of the channel (denoted by "1" and "0" respectively) obey exponential distribution with mean values $1/\lambda$ and $1/\mu$ respectively, at any time instant, the channel is busy with probability $p_B = \frac{\mu}{\lambda+\mu}$ and idle with probability $p_I = \frac{\lambda}{\lambda+\mu}$. Since the status transition can be modeled as alternating renewal process, the probability that the channel is in status ϕ given that it was in status θ ($\phi, \theta \in \{1, 0\}$) T_s seconds ago can thus be expressed as follows

$$\begin{aligned} p_{\theta\phi}(T_s) &= \begin{pmatrix} p_{00}(T_s) & p_{01}(T_s) \\ p_{10}(T_s) & p_{11}(T_s) \end{pmatrix} \\ &= \frac{1}{\lambda + \mu} \begin{pmatrix} \lambda + \mu e^{-(\lambda+\mu)T_s} & \mu - \mu e^{-(\lambda+\mu)T_s} \\ \lambda - \lambda e^{-(\lambda+\mu)T_s} & \mu + \lambda e^{-(\lambda+\mu)T_s} \end{pmatrix}. \end{aligned} \quad (8)$$

Therefore, the probabilities of the four hypotheses can be obtained by computing multi-step status transition probability and are expressed as follows

$$p_{H_0(x)} = p_I p_{00}^x(T_s) p_{01}(T_s) p_{11}^{J-x-1}(T_s), \quad 1 \leq x \leq I-1 \quad (9)$$

$$p_{H_1(x)} = \begin{cases} p_I p_{00}^x(T_s) p_{01}(T_s) p_{11}^{J-x-1}(T_s), & I \leq x \leq J-1 \\ p_I p_{00}^J(T_s), & x = J \end{cases} \quad (10)$$

$$p_{H_2(x)} = p_B p_{11}^x(T_s) p_{10}(T_s) p_{00}^{J-x-1}(T_s), \quad 1 \leq x \leq I-1 \quad (11)$$

$$p_{H_3(x)} = \begin{cases} p_B p_{11}^x(T_s) p_{10}(T_s) p_{00}^{J-x-1}(T_s), & I \leq x \leq J-1 \\ p_B p_{11}^J(T_s), & x = J \end{cases} \quad (12)$$

Since PU is essentially concerned with the interference probability rather than detection probability, we use interference probability to PU as the constraint in this paper as in [32]. The probability that at least one SU detects the channel as idle and transmits in hypothesis $H_i(x)$ can be derived as

$$P_{tr,H_i(x)} = 1 - \prod_{k=1}^K \left(1 - P_{tr,H_i(x)}^k\right). \quad (13)$$

Since packet based transmission is used in MAC, packet transmissions will fail due to collisions if there is any overlap between two or more concurrent transmissions. PU's transmission will be interfered if (i) PU's traffic is present in the data transmission period of SUs and (ii) at least one SU detects

the channel as idle and transmits. Therefore, the interference probability to PU can be expressed as

$$p_{in}(I, \varepsilon, J) = \sum_{x=1}^{I-1} p_{H_0(x)} p_{tr, H_0(x)} + \sum_{x=I}^{J-1} p_{H_1(x)} p_{tr, H_1(x)} + \sum_{x=I+1}^J p_{H_3(x)} p_{tr, H_3(x)}. \quad (14)$$

The probability that only SU_k detects the channel as idle and transmits and other SUs detect the channel as busy or choose not to transmit although they detect the channel as idle in hypothesis $H_i(x)$ can be expressed as

$$P_{s, H_i(x)}^k = P_{tr, H_i(x)}^k \cdot \prod_{\substack{m=1 \\ m \neq k}}^K (1 - P_{tr, H_i(x)}^m). \quad (15)$$

SU_k 's transmission will be successful if the following three conditions are all satisfied: (i) PU's traffic is absent in the data transmission period, (ii) SU_k detects the channel as idle and transmits with probability a , and (iii) other SUs detect the channel as busy or choose not to transmit. Therefore, SUs' average aggregated throughput for a long-term period can be expressed as

$$S(I, \varepsilon, J, \mathbb{P}) = \sum_{k=1}^K \left(p_{H_1(J)} p_{s, H_1(J)}^k G_{H_1(J)}^k + \sum_{x=1}^{I-1} p_{H_2(x)} p_{s, H_2(x)}^k G_{H_2(x)}^k + p_{H_3(I)} p_{s, H_3(I)}^k G_{H_3(I)}^k \right), \quad (16)$$

where $\mathbb{P} = (P_{tr}^1, P_{tr}^2, \dots, P_{tr}^K)$ represents SUs' transmission power vector.

Since the spectrum sensing power P_{se} mainly depends on the design of radio frequency front-end, it is considered as a fixed value for all SUs. On the contrary, SU_k 's data transmission power P_{tr}^k depends on its transmission probability. Thus, it is a variable and can be optimized. In the frame where SU_k detects the channel as idle and chooses to transmit, termed *Case A*, both spectrum sensing and data transmission are performed. Thus, SU_k 's energy consumption is $P_{se} \cdot IT_s + P_{tr}^k \cdot (J - I)T_s$. Otherwise, in the frame where SU_k detects the channel as busy or it chooses not to transmit when detecting the channel as idle, termed *Case B*, only spectrum sensing is performed. Thus, SU_k 's energy consumption is $P_{se} \cdot IT_s$.

The probability p_A^k of *Case A* for SU_k can be expressed as

$$p_A^k = \sum_{x=1}^{I-1} p_{H_0(x)} p_{tr, H_0(x)}^k + \sum_{x=I}^J p_{H_1(x)} p_{tr, H_1(x)}^k + \sum_{x=1}^{I-1} p_{H_2(x)} p_{tr, H_2(x)}^k + \sum_{x=I}^J p_{H_3(x)} p_{tr, H_3(x)}^k. \quad (17)$$

As *Case B* is the complementary set of *Case A*, the probability p_B^k of *Case B* for SU_k can be derived as

$$p_B^k = 1 - p_A^k. \quad (18)$$

Therefore, SU_k 's average power consumption for a long term can be expressed as follows

$$P_{ave}^k(I, \varepsilon, J, \mathbb{P}) = \frac{p_A^k (IP_{se} + (J - I)P_{tr}^k) + p_B^k IP_{se}}{J}. \quad (19)$$

From the derivation of the above three metrics, we observe that the heterogeneous fading channels do impact these three metrics by enabling SUs to use different sensing results, transmission probabilities and transmission rates.

In order to maximize SUs' aggregated throughput while satisfying the constraints of both interference probability to PU and SUs' average power consumption, the tradeoff problem is expressed as follows

$$\begin{aligned} & \max_{I, \varepsilon, J, \mathbb{P}} S(I, \varepsilon, J, \mathbb{P}), \\ & \text{s. t. (S1) } p_{in}(I, \varepsilon, J) \leq \bar{p}_{in}, \\ & \quad \quad \quad \text{(S2) } P_{ave}^k(I, \varepsilon, J, \mathbb{P}) \leq \bar{P}, \quad k \in \{1, 2, \dots, K\}, \end{aligned} \quad (20)$$

where \bar{p}_{in} and \bar{P} in constraints (S1) and (S2) denote the interference probability threshold and average power consumption threshold respectively.

To formulate the above problem, the path loss information, PU's transmission power and traffic distribution are required. In practical CRNs, the SUs can refer to the spectrum map [33], which records the time-varying spectrum condition within a specific area according to long-term statistics, for these information. And then, each SU includes these information into the routing packet and broadcasts the packet over CCC [20]. By exchanging the routing packets over CCC, each SU will obtain all these required information from its neighboring SUs. Finally, the cluster head of the distributed CRN can accomplish the formulation.

According to constraint (S1), I , ε and J jointly determine the interference probability to PU. Using bigger I and smaller ε increases the probability of detecting the channel as busy while using smaller J decreases the channel status changes. They both lead to a decrease of interference probability to PU. Similarly, I , ε , J and \mathbb{P} jointly determine SUs' aggregated throughput and each SU's transmission power. Therefore, we conclude that I , ε , J and \mathbb{P} are highly coupled in terms of their impact on the three metrics. This makes it challenging to compute the optimal combination of I , ε , J and \mathbb{P} to solve this optimization problem.

IV. HEURISTIC SOLUTION TO THE OPTIMIZATION PROBLEM

In the optimization problem, I and J are integers while ε and the elements of \mathbb{P} are continuous variables. Thus, the optimization problem is a mixed integer non-linear programming (MINLP) problem. Even if treating I and J as continuous variables, it is difficult to compute the partial derivatives of the target functions and constraints with respect to these unknown variables due to the complicated $Q(\cdot)$ function. This makes it challenging to compute the closed-form solution.

In this paper, by leveraging the convexity of the problem, a heuristic algorithm is proposed to lower the computational complexity. The heuristic algorithm consists of two parts: (1) the solution to Eq. (20) for a given pair of I and J : it computes

the optimal detection threshold and transmission power vector and then the corresponding SUs' aggregated throughput for the given pair of I and J ; and (2) the C-PSO algorithm: it computes the optimal combination of sensing duration and frame duration.

A. Solution for a Given Pair of I and J

Theorem 1: The optimal combination of I , ε , J and \mathbb{P} maximizing $S(I, \varepsilon, J, \mathbb{P})$ must guarantee that $p_{in}(I, \varepsilon, J) = \bar{p}_{in}$ and $P_{ave}^k(I, \varepsilon, J, \mathbb{P}) = \bar{P}$, $k \in \{1, 2, \dots, K\}$.

Proof: Proof by contradiction is used. Suppose that there exists an optimal solution denoted by $\{I_0, \varepsilon_0, J_0, \mathbb{P}_0\}$, which maximizes SUs' aggregated throughput while satisfying that $p_{in}(I_0, \varepsilon_0, J_0) < \bar{p}_{in}$ and $P_{ave}^k(I_0, \varepsilon_0, J_0, \mathbb{P}_0) < \bar{P}$, $k \in \{1, 2, \dots, K\}$. Here, \mathbb{P}_0 represents SUs' transmission power vector $(P_{tr,0}^1, P_{tr,0}^2, \dots, P_{tr,0}^K)$.

Let us consider the impact of detection threshold first. With the increase of detection threshold ε , SUs will be less likely to detect the channel as busy. Namely, SU $_k$'s detection probability $p_{d,H_i(x)}^k(I, \varepsilon)$ decreases with the increase of ε . This will allow SU $_k$ to transmit with a bigger transmission probability $p_{tr,H_i(x)}^k$ in the same hypothesis. Because the probability $p_{tr,H_i(x)}$ that at least one SU transmits increases with each SU's transmission probability, the increase of ε results in an increase of $p_{tr,H_i(x)}$. Thus, if a bigger detection threshold is used, SUs will cause more interference to PU based on Eq. (14). Indeed, we can conclude that we can choose a bigger detection threshold, i.e., $\varepsilon_1 > \varepsilon_0$, such that $p_{in}(I_0, \varepsilon_1, J_0) = p_{in}$. Meanwhile, since SUs' transmission probabilities, considering access contention, are smaller than $1/K$, the successful transmission probabilities $p_{s,H_i(x)}^k$ increases with the increase of SUs' transmission probabilities. Thus, we conclude that the chosen bigger detection threshold ε_1 results in an increase of SUs' aggregated throughput. Namely, $S(I_0, \varepsilon_1, J_0, \mathbb{P}_0) > S(I_0, \varepsilon_0, J_0, \mathbb{P}_0)$.

Further, based on Eq. (19), SU's average power consumption is monotonically increasing with its transmission power. We can thus choose a bigger transmission power for each SU so that SU's average power consumption equals the threshold \bar{P} . For example, $\mathbb{P}_1 = (P_{tr,1}^1, P_{tr,1}^2, \dots, P_{tr,1}^K)$ where $P_{tr,1}^k > P_{tr,0}^k$ can be chosen to guarantee that $P_{ave}^k(I_0, \varepsilon_1, J_0, \mathbb{P}_1) = \bar{P}$, $k \in \{1, 2, \dots, K\}$. Since each SU's achievable transmission rate is also monotonically increasing with its transmission power based on Eq. (6), SUs' aggregated throughput increases with the increase of SUs' transmission power. Therefore, we conclude that $S(I_0, \varepsilon_1, J_0, \mathbb{P}_1) > S(I_0, \varepsilon_1, J_0, \mathbb{P}_0)$.

According to the above derivation, we find that there exists another solution $\{I_0, \varepsilon_1, J_0, \mathbb{P}_1\}$, which results in $S(I_0, \varepsilon_1, J_0, \mathbb{P}_1) > S(I_0, \varepsilon_0, J_0, \mathbb{P}_0)$ while satisfying $p_{in}(I_0, \varepsilon_1, J_0) = \bar{p}_{in}$ and $P_{ave}^k(I_0, \varepsilon_1, J_0, \mathbb{P}_1) = \bar{P}$, $k \in \{1, 2, \dots, K\}$. This finding is contradictory to the previous supposition that $\{I_0, \varepsilon_0, J_0, \mathbb{P}_0\}$ maximizes SUs' throughput. Therefore, Theorem 1 is proven. ■

Applying Theorem 1, two inequality constraints can be transformed into equality constraints and then the optimization problem can be redefined as follows

$$\max_{I, \varepsilon, J, \mathbb{P}} S(I, \varepsilon, J, \mathbb{P}),$$

Algorithm 1: Solution to Eq. (20) for Given I and J

- 1: **Input:** d_k , ($1 \leq k \leq K$), α and the given I and J .
 - 2: Derive the expressions of interference probability to PU, SUs' aggregated throughput and average power consumption respectively as function of ε and \mathbb{P} .
 - 3: Compute optimal detection threshold ε^* by solving constraint (S3)
 - 4: Substitute ε^* into $P_{ave}^k(I, \varepsilon, J, \mathbb{P})$ and then compute SUs' optimal transmission power vector \mathbb{P}^* by solving constraint (S4).
 - 5: Compute maximal SUs' aggregated throughput S^* by substituting ε^* and \mathbb{P}^* into $S(I, \varepsilon, J, \mathbb{P})$.
 - 6: **Output:** ε^* and \mathbb{P}^* are the optimal solution for the given pair of I and J while S^* is the corresponding maximum throughput.
-

$$\text{s. t. (S3) } p_{in}(I, \varepsilon, J) = \bar{p}_{in},$$

$$(S4) P_{ave}^k(I, \varepsilon, J, \mathbb{P}) = \bar{P}, \quad k \in \{1, 2, \dots, K\}. \quad (21)$$

For a given pair of I and J , the detection threshold ε can be computed via constraint (S3) using numerical techniques. Then, substituting the computed detection threshold into constraint (S4), we can compute each SU's optimal transmission power. Therefore, we propose Algorithm 1 to solve the optimization problem for given I and J .

If the optimal detection threshold and transmission power vector are denoted by ε^* and \mathbb{P}^* respectively, the optimization problem can be transformed into an integer non-linear programming problem as

$$\max_{I, J} S(I, J) \triangleq S(I, \varepsilon^*, J, \mathbb{P}^*). \quad (22)$$

B. Cluster Based Particle Swarm Optimization (C-PSO)

In this paper, since I and J should be jointly optimized, the exhaustive search algorithm [10] is not effective. Considering the fact that both I and J are integers, we can vary their values under different conditions and obtain the relation between SUs' aggregated throughput, I and J .

Fig. 2 shows SUs' aggregated throughput variation with I and J for different distances from PU to SUs, different PU's traffic distributions and different numbers of SUs. We observe that for a fixed value of J , SUs' aggregated throughput increases with I until it reaches its peak and then decreases. Moreover, for a fixed value of I , SUs' aggregated throughput increases with J until it reaches its peak and then decreases. Therefore, we can conclude that $S(I, J)$ is unimodal in the solution space. Owing to the special relation between SUs' aggregated throughput, I and J , a cluster based particle swarm optimization (C-PSO) algorithm is proposed to efficiently solve the problem defined by Eq. (22). The C-PSO algorithm resembles climbing a mountain. By observing the surrounding altitude and then moving to the higher place, the climber can gradually and efficiently approach the mountaintop. The details of the algorithm can be explained as follows.

According to C-PSO, a pair of I and J represents a particle, i.e., $y_t = (I_t, J_t)$ in t th iteration, and the corresponding SUs'

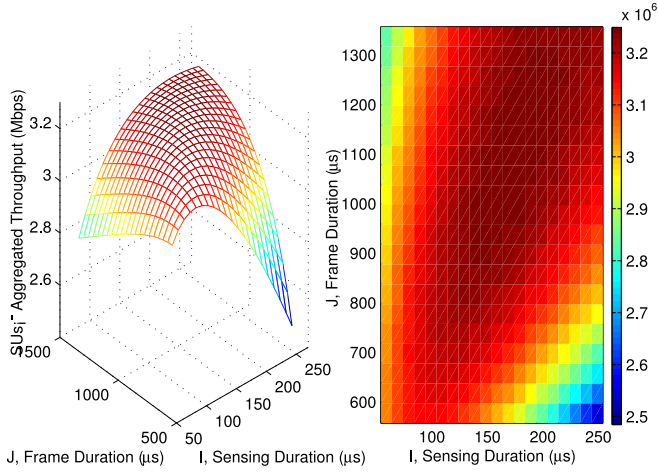
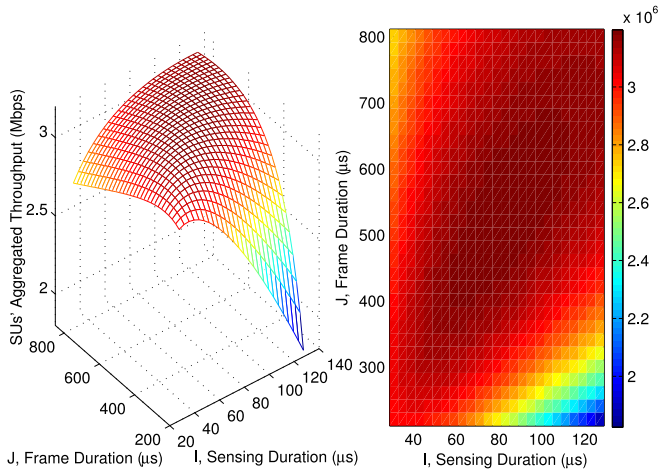
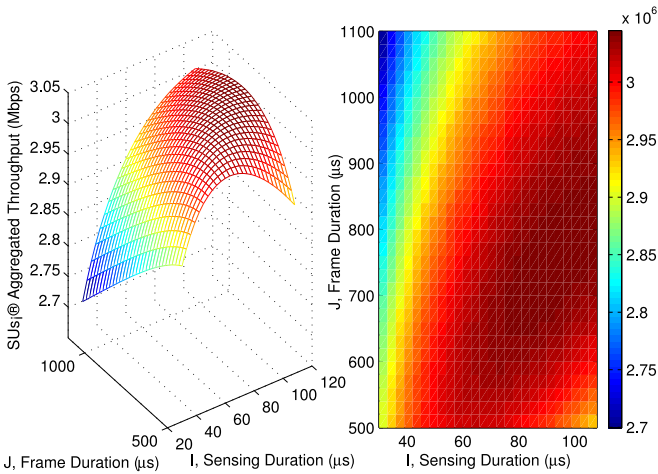
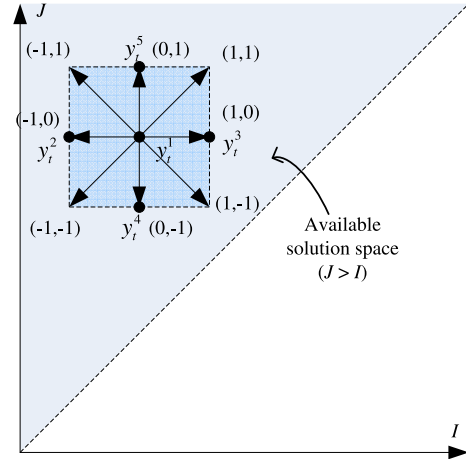

 (a) $\bar{d} = 600m$, $\lambda = \mu = 100$, $K = 30$

 (b) $\bar{d} = 500m$, $\lambda = \mu = 200$, $K = 30$

 (c) $\bar{d} = 500m$, $\lambda = \mu = 100$, $K = 20$

 Fig. 2. Variation of SUs' aggregated throughput $S(I, J)$ with I and J under different conditions.

aggregated throughput $S(y_t) = S(I_t, J_t)$ is the fitness function. The best known particle g_{best_t} is defined as the particle with biggest fitness searched until t th iteration. Since J should be


 Fig. 3. Diagram of C-PSO, where 5 black dots represent the particles in the cluster and (a, b) close to the arrow represents the potential direction factor.

bigger than I , the available solution space is $\mathbb{O} = \{I, J | J > I > 0\}$. Our goal is to find a solution y^* to satisfy $S(y^*) \geq S(y_t)$ for all y_t in the solution space, which means that y^* is the global maximum.

C-PSO consists of 3 phases: (1) one particle is randomly chosen from \mathbb{O} and then the other 4 neighbouring particles are generated. A cluster composed of these 5 particles is initialized; (2) the velocity is updated, jointly considering the comparison of the fitnesses of these 5 particles and the best known particle. Then, 5 particles are updated using this velocity; and (3) the fitnesses of 5 updated particles are computed and then the best known particle is updated based on the comparison of the computed fitnesses against the previous best known particle. Iteratively using the second and third phases, we can obtain the optimal particle with biggest fitness. The details of C-PSO are described as follows.

Phase 1: Randomly choose one particle and initialize the cluster.

Instead of using particles randomly distributed in the solution space and independent velocity for each individual particle in traditional PSO algorithms [34], we employ a cluster composed of 5 neighbouring particles $\mathbb{Y}_t = \{y_t^1, y_t^2, \dots, y_t^5\}$ and a common velocity v_t for all 5 particles in the cluster. As shown in Fig. 3, the 5 particles are defined as $y_t^1 = (I_t, J_t)$, $y_t^2 = (I_t - 1, J_t)$, $y_t^3 = (I_t + 1, J_t)$, $y_t^4 = (I_t, J_t - 1)$ and $y_t^5 = (I_t, J_t + 1)$ respectively. Note that the superscript represents the relative position of the particle in the cluster while the subscript represents the number of iteration. We let $S(\mathbb{Y}_t) = \{S(y_t^1), S(y_t^2), \dots, S(y_t^5)\}$ denote the fitnesses of the particles in a cluster.

First, one particle denoted by $y_0^1 = (I_0, J_0)$ is randomly chosen from \mathbb{O} , i.e., $y_0^1 \in \mathbb{O}$. y_0^1 is regarded as the central particle and other 4 neighbouring particles are generated. One cluster \mathbb{Y}_0 composed of these 5 neighbouring particles is initialized. The fitnesses of these 5 particles are computed based on Algorithm 1. The particle with biggest fitness is chosen as g_{best_0} . The initial velocity v_0 is set to $(0, 0)$.

Phase 2: Update velocity and particles of the cluster.

Apart from current velocity v_t , velocity v_{t+1} in the next iteration is determined by: (i) the comparison among the elements

TABLE I
ASSIGNMENT OF DIRECTION FACTOR (a, b)

Condition	Value of a	Condition	Value of b
$S(y_t^2) < S(y_t^1) < S(y_t^3)$	+1	$S(y_t^4) < S(y_t^1) < S(y_t^5)$	+1
$S(y_t^2) > S(y_t^1) > S(y_t^3)$	-1	$S(y_t^4) > S(y_t^1) > S(y_t^5)$	-1
$S(y_t^2) < S(y_t^1), S(y_t^1) > S(y_t^3)$	0	$S(y_t^4) < S(y_t^1), S(y_t^1) > S(y_t^5)$	0

in $S(\mathbb{Y}_t)$, and (ii) the direction from the central particle y_t^1 to the best known particle g_{best_t} , i.e., $g_{best_t} - y_t^1$. The details are explained as follows.

Considering the fact that $S(I, J)$ increases with both I and J until it reaches the peak and then decreases, we define a direction factor (a, b) , rather than using each particle's individual maximum, to decide the trajectory of the cluster. The value of direction factor is computed based on the comparison among the elements in $S(\mathbb{Y}_t)$ using the criterion shown in Table I. Specifically, the horizontal direction factor a depends on the comparison among $\{S(y_t^1), S(y_t^2), S(y_t^3)\}$ while the vertical direction factor b depends on the comparison among $\{S(y_t^1), S(y_t^4), S(y_t^5)\}$. Therefore, direction factor (a, b) keeps the cluster moving towards the particles with greater fitnesses both horizontally and vertically. Moreover, the direction $g_{best_t} - y_t^1$ pulls the cluster to the best known particle.

After velocity v_{t+1} is computed, the particles are updated. Therefore, we update the velocity and the particles of the cluster as follows

$$v_{t+1} = \omega \cdot v_t + rand \cdot c_1 \cdot (a, b) + rand \cdot c_2 \cdot (g_{best_t} - y_t^1),$$

$$y_{t+1}^n = round(y_t^n + v_{t+1}^n), \quad n \in \{1, 2, \dots, 5\}, \quad (23)$$

where ω is the inertia weight, $round(\cdot)$ returns the nearest integer, $rand$ returns a value randomly chosen between 0 and 1, and c_1 and c_2 are acceleration vectors that pull the cluster towards the direction factor and $g_{best_t} - y_t^1$.

Phase 3: Compute fitnesses and update the best known particle.

After updating the particles of the cluster, the fitness values of all particles in the new cluster, i.e., $S(\mathbb{Y}_{t+1})$, are computed using Algorithm 1. Comparing the maximum fitness among the elements in $S(\mathbb{Y}_{t+1})$ against g_{best_t} , we update the best known particle as follows

$$g_{best_{t+1}} = \begin{cases} g_{best_t}, & S(g_{best_t}) \geq \max\{S(\mathbb{Y}_{t+1})\}, \\ \arg \max_{y_{t+1}^n \in \mathbb{Y}_{t+1}} \{S(y_{t+1}^n)\}, & \text{otherwise,} \end{cases} \quad (24)$$

The particles in the cluster \mathbb{Y}_t , common velocity v_t and the best known particle g_{best_t} are updated in each iteration. As $S(I, J)$ is unimodal, the iteration continues unless $S(y_t^1)$ becomes the maximum value in the cluster. The convergence is guaranteed by the convexity property of $S(I, J)$. The whole procedure of the solution to the optimization problem can be summarized as shown in Algorithm 2.

V. SIMULATION RESULTS AND DISCUSSIONS

In this section, the impact of heterogeneous fading channels is evaluated via network simulations. In the simulations, 30 SUs are randomly located within a single-hop area, i.e.,

Algorithm 2: C-PSO Algorithm for the Tradeoff Problem

- 1: Randomly choose one particle y_0^1 as the central particle and then initialize the cluster \mathbb{Y}_0 .
- 2: **while** $S(y_t^1) \neq \max\{S(\mathbb{Y}_t)\}$ **do**
- 3: Update v_{t+1} and \mathbb{Y}_{t+1} using Eq. (23).
- 4: Compute the fitness $S(\mathbb{Y}_{t+1})$ using Algorithm 1, and update the best known particle $g_{best_{t+1}}$ using Eq. (24).
- 5: **end while**
- 6: **Output:** g_{best_t} is the optimal combination of I and J while $S(g_{best_t})$ is the corresponding maximum SUs' aggregated throughput.

TABLE II
SIMULATION PARAMETERS AND VALUES

Description	Value
Number of SUs K	30
Available bandwidth B	1MHz
Sampling interval T_s	1 μ s
Working frequency f	800MHz
Conditional access probability a	0.1
Interference probability threshold P_{in}	0.1
Spectrum sensing power P_{se}	10dBm
Power consumption threshold P	20dBm
PU's transmission power P_{pu}	35dBm
Variance of Gaussian noise N_0	-40dBm
Inertia weight ω	(0.8, 0.8) ^T
Acceleration vectors c_1, c_2	(1, 1) ^T

a circle of 250-meter radius, such that their path losses are different. The distance from the center of this circle to PU is denoted by \bar{d} . Considering the fact that 802.22 WRANs work over TV "white space" [35], we set the working frequency f to 800MHz. We consider the scenario of under-utilized PU's traffic. More specifically, the channel is idle and busy with the same probability, i.e., $\lambda = \mu$. Other simulation parameters are shown in Table II. For comparison, we compute SUs' throughput and interference probability to PU in related contributions [10]–[12] which assume homogeneous fading channel, i.e., all SUs are exposed to the same fading channel. More specifically, we study two schemes: (1) *aggressive scheme* and (2) *conservative scheme*. Aggressive scheme considers that all SUs are exposed to the smallest path loss and thus receive strongest PU's signal; on the contrary, conservative scheme considers that all SUs are exposed to the biggest path loss and thus receive weakest PU's signal.

A. Feasibility of C-PSO

We set C-PSO parameters to fixed values, i.e., $\omega = (0.8, 0.8)^T$ and $c_1 = c_2 = (1, 1)^T$. Indeed, by using adaptive

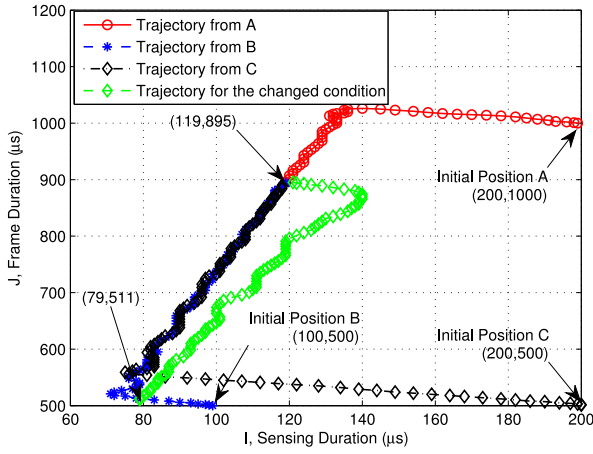
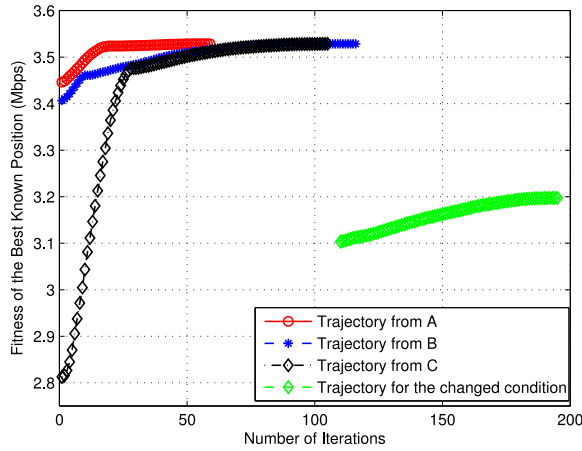

 (a) Trajectory of the best known particle g_{best_t} .

 (b) Trajectory of SU's aggregated throughput $S(g_{best_t})$.

Fig. 4. The convergence of C-PSO iterative algorithm.

parameters proposed in [36], the convergence speed can be accelerated, which is omitted here in order to highlight our focus. In the simulations, the initial condition of the CRN is the same as in Table II, and then the PU's traffic distribution parameter changes from $\lambda = \mu = 100$ to $\lambda = \mu = 200$. Therefore, each algorithm needs to run twice: one run for the initial condition and one run for the changed condition.

We consider three initial central particles randomly chosen from \mathbb{O} . They are $(200, 1000)$ represented by A, $(100, 500)$ represented by B and $(200, 500)$ represented by C. Fig. 4(a) shows the trajectory of g_{best_t} , while Fig. 4(b) shows the corresponding SU's aggregated throughput $S(g_{best_t})$ starting from the above three initial particles A, B and C when $\lambda = \mu = 100$ and $\bar{d} = 500\text{m}$. More specifically, for the first optimization, the best known particle g_{best_t} converges to $(119, 895)$ after 59 iterations from position A, after 110 iterations from position B and after 106 iterations from position C. The maximum SU's aggregated throughput is 3.5285Mbps . For the second optimization, the best known particle g_{best_t} moves from the prior optimal particle $(119, 895)$ to $(79, 511)$ after 79 iterations. When PU's traffic distribution changes, the fitness drops to 3.1042Mbps ; during the optimization procedure, the fitness

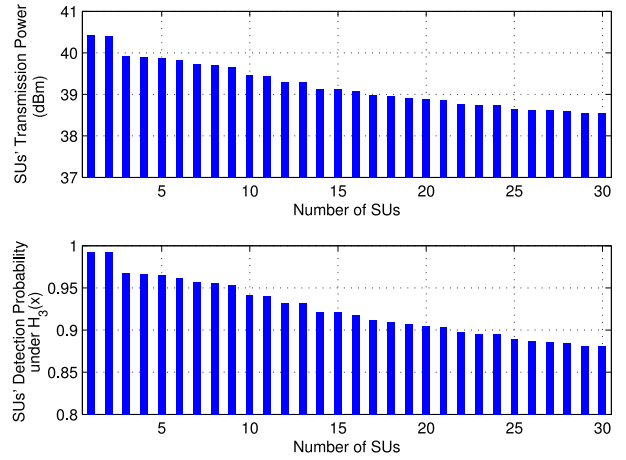
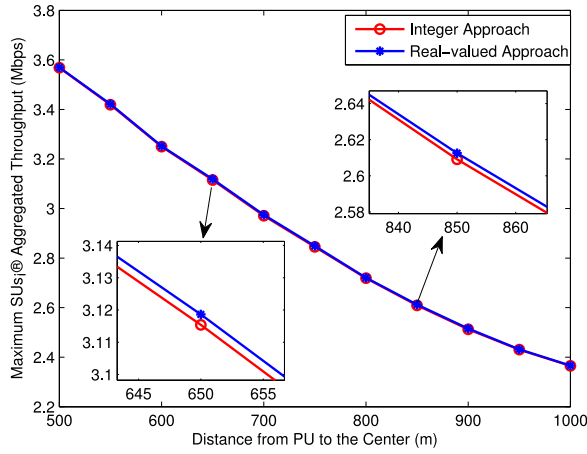


Fig. 5. The impact of heterogeneous fading channels on SU's optimal transmission power and SU's detection probability.

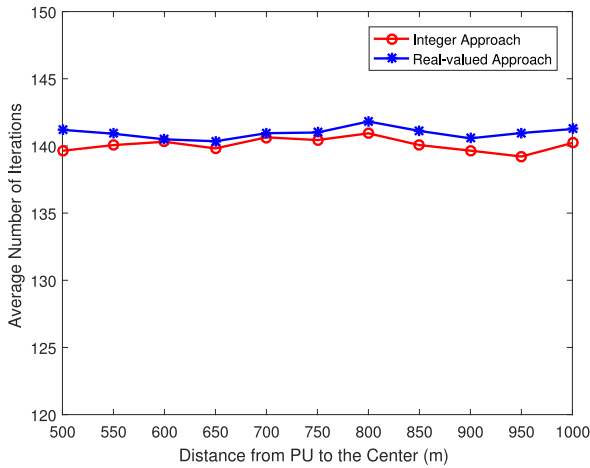
gradually improves, achieving the maximum 3.2013Mbps . This figure indicates that our proposed C-PSO can solve the tradeoff problem effectively despite the randomly chosen initial particles. From Fig. 4(b), we observe that using the optimized parameters settings can improve SU's aggregated throughput performance compared against using the initial parameters. Moreover, the algorithm can converge to the new optimal solution if the wireless environment changes. Namely, the proposed C-PSO algorithm can adapt to the time-varying wireless environment.

Using the optimal I and J , we compute each SU's optimal transmission power and detection probabilities under $H_3(x)$ for the initial condition as shown in Fig. 5 respectively. SUs are sorted in the descending order of the distance from SUs to PU. We observe that 30 SUs do have different detection probabilities and use different transmission powers due to heterogeneous fading channels. SUs closer to PU are exposed to smaller path loss and thus their detection probabilities are bigger. These SUs transmit with smaller transmission probabilities. This leads to more remaining energy and higher transmission power. These simulation results illustrate the significance of our study on the impact of heterogeneous fading channels in power limited CRNs.

In this paper, since I and J are assumed integers, the distance between the central particle and its neighbors in the cluster equals 1, and *round* function is used in Eq. (23) to ensure that I and J are integers. Indeed, real-valued approach can also be used; we just need to shorten the distance between the central particle and its neighbors to a proper fraction (i.e., shorten the distance from 1 to 0.1) and not use *round* function to unintigerize the positions of particles. After computing the real-valued solution, denoted by I' and J' , we compare the throughput of its four neighbors $((\lfloor I' \rfloor, \lfloor J' \rfloor), (\lfloor I' \rfloor, \lceil J' \rceil), (\lceil I' \rceil, \lfloor J' \rfloor), (\lceil I' \rceil, \lceil J' \rceil))$ to obtain the optimal integer solution. Fig. 6 shows the throughput performance and the average number of iterations of integer and real-valued approaches while varying with the distance \bar{d} from PU to the center of SUs. The comparison shows that both the performance gap and the time complexity difference between



(a) The optimal SUs' aggregated throughput.



(b) The average number of iterations.

Fig. 6. Comparison of the integer and real-valued approaches while varying with the distance from PU to the center.

these two approaches are negligible. Thus, the simulations show that the integer approach is feasible to solve the problem.

As for the computational complexity of the C-PSO algorithm, in each iteration, the fitness of the 5 particles in the cluster is computed; and then, the particles and the velocity are updated. Since the computational complexity of updating is much lower than that of computing the fitness, the computational complexity of the proposed algorithm can be measured by the number of fitness computations. The problem defined by Eq. (20) can be solved by numerical technique, as shown in Algorithm 1, the computational complexity of one particle's fitness computation can be regarded as a fixed value C . If the number of required iterations before the convergence is N_{ite} , the computational complexity can be written as $\Omega(5N_{ite}C)$, where $\Omega(\cdot)$ is the Big-Omega notation. We note that the computational complexity of the proposed algorithm depends only on the number of required iterations before the convergence of the algorithm. The complexity is irrelevant to the number of SUs and the channel conditions. Moreover, the complexity of the algorithm is a linear function with respect to the complexity of one particle's fitness computation C . Thus, the computational complexity of the proposed algorithm is low.

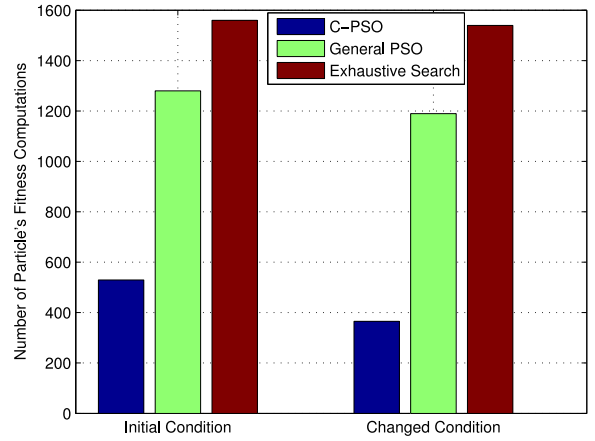


Fig. 7. The average number of particle's fitness computations using the C-PSO, exhaustive search and general PSO algorithms.

In the following, we compare the computational complexity of the proposed algorithm with those of other algorithms, including the exhaustive search (binary search on I and J) [10], [12] and the general PSO (5 randomly selected particles, rather than 5 adjacent particles) [37]. The simulations run 100 times and the average number of particle's fitness computations for the two conditions is shown in Fig. 7. It can be observed that the number of required computations for C-PSO is much smaller than those for exhaustive search and general PSO. This is because, for C-PSO, the moving direction of the cluster can be controlled by the comparison of the fitness of the particles in the cluster. By leveraging the convexity of the problem, the convergence procedure is accelerated and thus the number of required iterations decreases. Moreover, for the C-PSO algorithm, the number for the changed condition is smaller than that for the initial condition. This can be explained as follows. Under the initial condition, the initial central particle is randomly chosen in the solution space \mathbb{O} , which may be far away from the optimal particle. But, under the changed condition, the initial central particle is the optimal particle computed under the initial condition, i.e., (119, 895). In this case, the number of required iterations before reaching the new optimal particle (79, 511) may be smaller, especially when the distance between the prior optimal particle and the new optimal particle is small. From the above simulations, we can observe that if the wireless environment changes, the algorithm can converge to the new optimal solution after smaller number of iterations. Namely, the proposed C-PSO algorithm can adapt to the time-varying wireless environment.

In the above simulations, even if fixed C-PSO parameters are used, the computational complexity is lower. When adaptive parameters proposed in existing contributions [36], [37], which focus on the optimization of PSO algorithm, are used, the number of iterations can be further decreased. Considering the first application of the C-PSO algorithm in CRNs and the resulting complexity decrease, we advocate that the C-PSO algorithm is an important innovation. As for the further optimization of the C-PSO algorithm, various methods have been proposed to accelerate the convergence. Some methods may be integrated to our proposal to make the algorithm

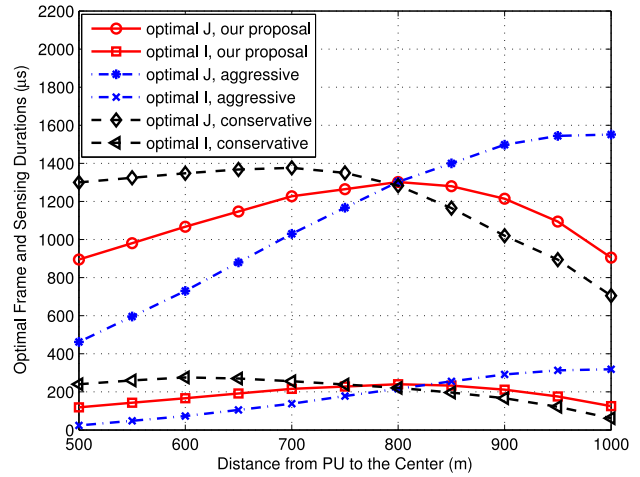
more efficient. We plan to study it from the engineering perspective as a future work.

B. Impact of Heterogeneous Fading Channels

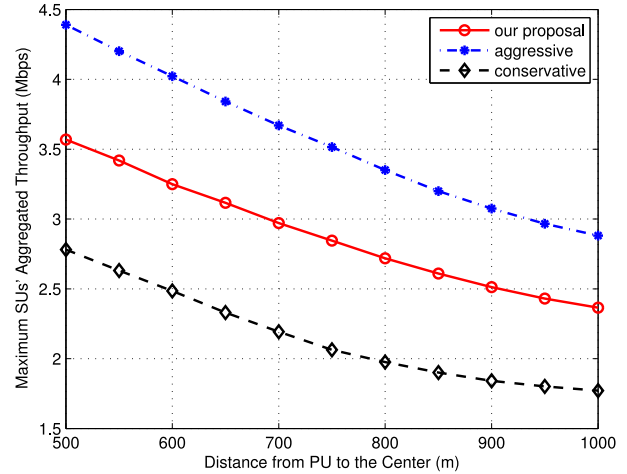
Considering the fact that path loss is highly related to the distance from SU to PU, we change the value of \bar{d} and evaluate the impact of heterogeneous fading channels from PU to SUs on the tradeoff problem. We also compare both the SUs' throughput and interference probability to PU performance between our proposal (considering heterogeneous fading channel) and related contributions (considering homogeneous fading channel).

Fig. 8 shows the variation of optimal sensing duration and frame duration (a), maximum SUs' aggregated throughput (b) and interference probability to PU (c) respectively with the distance \bar{d} when $\lambda = \mu = 100$. We observe that SUs' aggregated throughput decreases with the increase of \bar{d} . Meanwhile, the optimal sensing and frame durations increase with \bar{d} until they reach the climax and then they decrease. The simulation results can be explained by the fact that the distance \bar{d} impacts SUs' throughput from two aspects. On one hand, path loss increases with \bar{d} and thus PU's signal received by SUs becomes weaker. This makes it more difficult for SUs to detect the channel status. Therefore, SUs have to use higher ratio of sensing duration and bigger detection threshold to satisfy the interference probability constraint. Then, SUs get less transmission opportunities and their throughput decreases. On the other hand, the decrease of PU's signal indicates that the interference to SUs' transmission decreases and SUs' transmission rate increases. The decrease of SUs' throughput caused by the former aspect exceeds the increase of SUs' throughput caused by the latter aspect. Therefore, maximum SUs' aggregated throughput decreases with the increase of \bar{d} .

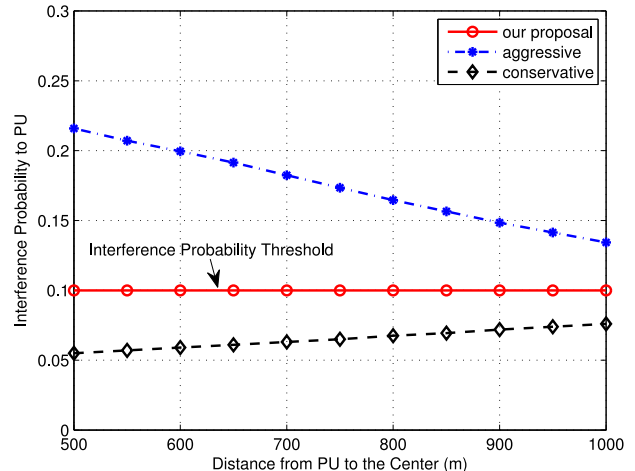
We compare SUs' aggregated throughput and interference probability to PU obtained by our proposal and the two schemes. We observe that our proposal outperforms conservative scheme in terms of SUs' aggregated throughput but underperforms conservative scheme in terms of the interference probability to PU. This can be explained by the fact that the conservative scheme pessimistically considers the path loss and it assumes that all SUs are receiving weakest PU's signal. Thus, SUs use overly high ratio of sensing duration to guarantee the interference probability constraint, causing more power consumption in sensing period. Both the relative increase of sensing duration and the increase of power consumption for spectrum sensing decrease the throughput performance. But, the overly high ratio of sensing duration increases the probability of detecting the channel as busy. This decreases SUs' transmission probabilities and thus the interference probability to PU is smaller than the interference probability threshold. We also observe that our proposal underperforms aggressive scheme in terms of SUs' aggregated throughput but outperforms aggressive scheme in terms of the interference probability to PU. More importantly, the interference probability to PU obtained by aggressive scheme exceeds the threshold which is not acceptable. This can be explained by the fact that aggressive scheme optimistically considers the path loss and



(a) Optimal sensing duration and frame duration.



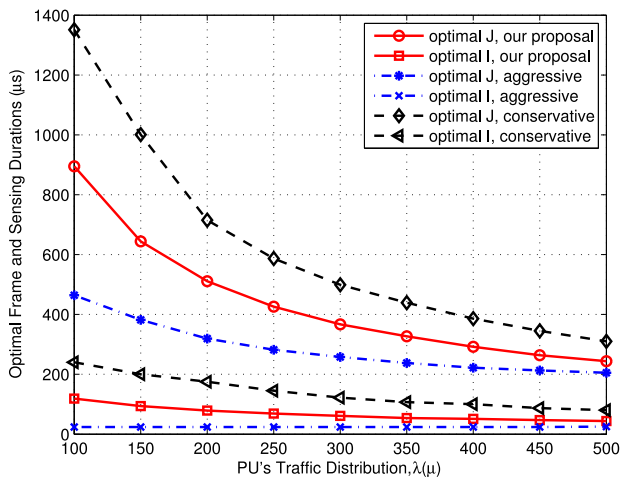
(b) Maximum SUs' aggregated throughput.



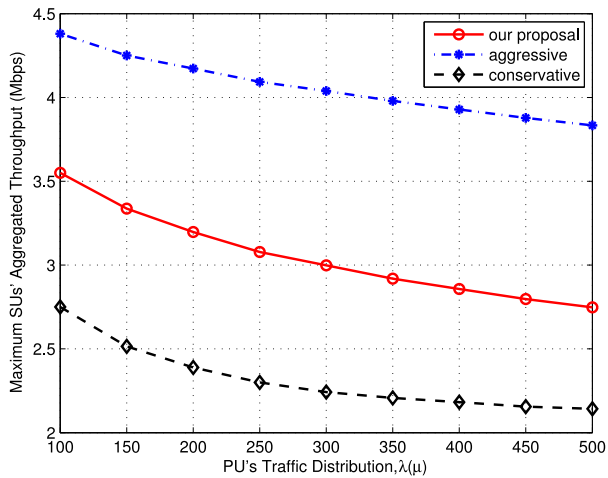
(c) Interference probability to PU.

Fig. 8. Impact of \bar{d} on the tradeoff.

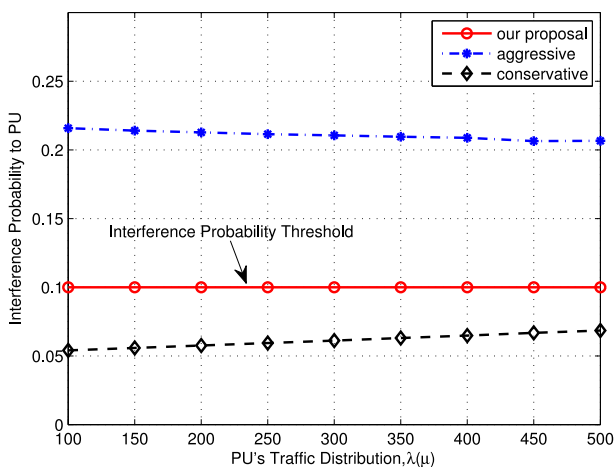
it assumes that all SUs are receiving strongest PU's signal. Then, SUs use lower ratio of sensing duration. The reliability of spectrum sensing decreases and SUs get more chances



(a) Optimal sensing duration and frame duration.



(b) Maximum SUs' aggregated throughput.



(c) Interference probability to PU.

Fig. 9. Impact of PU's traffic distribution on the tradeoff.

to detect the channel as idle. Thus, the interference probability to PU exceeds the threshold, although the throughput performance is improved to some extent. Therefore, we conclude that the solution obtained by our proposal can achieve

the maximum throughput performance while strictly satisfying the interference probability to PU constraint.

C. Impact of PU's Traffic Distribution

Fig. 9 shows the variation of optimal sensing duration and frame duration (a), maximum SUs' aggregated throughput (b) and interference probability to PU (c) respectively with λ when $\bar{d} = 500\text{m}$. We observe that both the optimal sensing duration and frame duration decrease with the increase of λ while the throughput performance decreases with λ . This can be explained by the fact that with the increase of λ , the average idle or busy status of the channel, namely $1/\lambda$, becomes shorter, which implies that the channel status changes more frequently and thus SUs' transmissions are more likely to collide with PU's traffic. Thus, SUs have to decrease frame duration and increase the ratio of sensing duration to ensure the interference probability constraint, which obviously degrades the throughput performance. We also observe that the throughput performance of our proposal is better than that of conservative scheme but worse than that of aggressive scheme. The reason has been discussed in previous subsection.

From Figs. 8 and 9, we can conclude that the solution of the tradeoff problem varies with both the heterogeneous fading channels and PU's traffic distribution. Therefore, the sensing duration, frame duration, detection threshold and transmission power vector should be carefully designed factoring these two conditions for improved performance.

VI. CONCLUSION

In this paper, the impact of heterogeneous fading channels on the performance of power limited CRNs is studied in the presence of the tradeoff between the interference probability to PU and SUs' aggregated throughput. The sensing duration, frame duration, detection threshold and transmission power are jointly optimized via our proposed C-PSO algorithm for an improved SUs' throughput performance under interference probability and power consumption constraints. Simulation results validate the outperformance of our proposal compared to related contributions which assume that all SUs suffer from the same channel fading.

REFERENCES

- [1] S. Bhattarai, J.-M. J. Park, B. Gao, K. Bian, and W. Lehr, "An overview of dynamic spectrum sharing: Ongoing initiatives, challenges, and a roadmap for future research," *IEEE Trans. Cogn. Commun. Netw.*, vol. 2, no. 2, pp. 110–128, Jun. 2016.
- [2] S. Stotas and A. Nallanathan, "On the throughput and spectrum sensing enhancement of opportunistic spectrum access cognitive radio networks," *IEEE Trans. Wireless Commun.*, vol. 11, no. 1, pp. 97–107, Jan. 2012.
- [3] V. Wong, R. Schober, D. Ng, and L. Wang, *Key Technologies for 5G Wireless Systems*. Cambridge, U.K.: Cambridge Univ. Press, 2017.
- [4] B. Ma, M. H. Cheung, V. W. S. Wong, and J. Huang, "Hybrid overlay/underlay cognitive femtocell networks: A game theoretic approach," *IEEE Trans. Wireless Commun.*, vol. 14, no. 6, pp. 3259–3270, Jun. 2015.
- [5] E. C. Y. Peh, Y.-C. Liang, Y. L. Guan, and Y. Zeng, "Optimization of cooperative sensing in cognitive radio networks: A sensing-throughput tradeoff view," *IEEE Trans. Veh. Technol.*, vol. 58, no. 9, pp. 5294–5299, Nov. 2009.

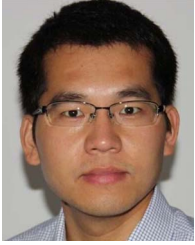
- [6] Y.-C. Liang, Y. Zeng, E. C. Y. Peh, and A. T. Hoang, "Sensing-throughput tradeoff for cognitive radio networks," *IEEE Trans. Wireless Commun.*, vol. 7, no. 4, pp. 1326–1337, Apr. 2008.
- [7] J. Zhang, F.-C. Zheng, X.-Q. Gao, and H.-B. Zhu, "Sensing-energy efficiency tradeoff for cognitive radio networks," *IET Commun.*, vol. 8, no. 18, pp. 3414–3423, Dec. 2014.
- [8] W. Zhang and C. K. Yeo, "Joint iterative algorithm for optimal cooperative spectrum sensing in cognitive radio networks," *Comput. Commun.*, vol. 36, no. 1, pp. 80–89, Dec. 2012.
- [9] L. Tang, Y. Chen, E. L. Hines, and M.-S. Alouini, "Effect of primary user traffic on sensing-throughput tradeoff for cognitive radios," *IEEE Trans. Wireless Commun.*, vol. 10, no. 4, pp. 1063–1068, Apr. 2011.
- [10] S. Zhang, H. Zhao, S. Wang, and J. Wei, "A cross-layer rethink on the sensing-throughput tradeoff for cognitive radio networks," *IEEE Commun. Lett.*, vol. 18, no. 7, pp. 1226–1229, Jul. 2014.
- [11] S. Zhang, A. S. Hafid, H. Zhao, and S. Wang, "Cross-layer rethink on sensing-throughput tradeoff for multi-channel cognitive radio networks," *IEEE Trans. Wireless Commun.*, vol. 15, no. 10, pp. 6883–6897, Oct. 2016.
- [12] S. Zhang, A. S. Hafid, H. Zhao, and S. Wang, "Cross-layer aware joint design of sensing and frame durations in cognitive radio networks," *IET Commun.*, vol. 10, no. 9, pp. 1111–1120, Jun. 2016.
- [13] A. Celik and A. E. Kamal, "Multi-objective clustering optimization for multi-channel cooperative spectrum sensing in heterogeneous green CRNs," *IEEE Trans. Cogn. Commun. Netw.*, vol. 2, no. 2, pp. 150–161, Jun. 2016.
- [14] D. W. K. Ng, E. S. Lo, and R. Schober, "Multiobjective resource allocation for secure communication in cognitive radio networks with wireless information and power transfer," *IEEE Trans. Veh. Technol.*, vol. 65, no. 5, pp. 3166–3184, May 2016.
- [15] S. Senthilmurugan and T. G. Venkatesh, "Optimal channel sensing strategy for cognitive radio networks with heavy-tailed idle times," *IEEE Trans. Cogn. Commun. Netw.*, vol. 3, no. 1, pp. 26–36, Mar. 2017.
- [16] H. Pradhan, S. S. Kalamkar, and A. Banerjee, "Sensing-throughput tradeoff in cognitive radio with random arrivals and departures of multiple primary users," *IEEE Commun. Lett.*, vol. 19, no. 3, pp. 415–418, Mar. 2015.
- [17] X. Xing *et al.*, "Optimal spectrum sensing interval in cognitive radio networks," *IEEE Trans. Parallel Distrib. Syst.*, vol. 25, no. 9, pp. 2408–2417, Sep. 2014.
- [18] Y. Chen and H.-S. Oh, "A survey of measurement-based spectrum occupancy modeling for cognitive radios," *IEEE Commun. Surveys Tuts.*, vol. 18, no. 1, pp. 848–859, 1st Quart., 2016.
- [19] J. Zhang, L. Qi, and H. Zhu, "Optimization of MAC frame structure for opportunistic spectrum access," *IEEE Trans. Wireless Commun.*, vol. 11, no. 6, pp. 2036–2045, Jun. 2012.
- [20] A. Celik, A. Alsharoa, and A. E. Kamal, "Hybrid energy harvesting-based cooperative spectrum sensing and access in heterogeneous cognitive radio networks," *IEEE Trans. Cogn. Commun. Netw.*, vol. 3, no. 1, pp. 238–248, Mar. 2017.
- [21] A. Celik and A. E. Kamal, "Green cooperative spectrum sensing and scheduling in heterogeneous cognitive radio networks," *IEEE Trans. Cogn. Commun. Netw.*, vol. 2, no. 3, pp. 238–248, Sep. 2016.
- [22] N. Nguyen-Thanh, P. Ciblat, S. Maleki, and V.-T. Nguyen, "How many bits should be reported in quantized cooperative spectrum sensing?" *IEEE Wireless Commun. Lett.*, vol. 4, no. 5, pp. 465–468, Oct. 2015.
- [23] S. Hussain and X. N. Fernando, "Performance analysis of relay-based cooperative spectrum sensing in cognitive radio networks over non-identical Nakagami- m channels," *IEEE Trans. Commun.*, vol. 62, no. 8, pp. 2733–2746, Aug. 2014.
- [24] A. Afana, T. M. N. Ngatched, and O. A. Dobre, "Cooperative AF relaying with beamforming and limited feedback in cognitive radio networks," *IEEE Commun. Lett.*, vol. 19, no. 3, pp. 491–494, Mar. 2015.
- [25] F. Moghimi, R. K. Mallik, and R. Schober, "Sensing time and power optimization in MIMO cognitive radio networks," *IEEE Trans. Wireless Commun.*, vol. 11, no. 9, pp. 3398–3408, Sep. 2012.
- [26] S. Yin, Z. Qu, and S. Li, "Achievable throughput optimization in energy harvesting cognitive radio systems," *IEEE J. Sel. Areas Commun.*, vol. 33, no. 3, pp. 407–422, Mar. 2015.
- [27] Y. Liu, S. Xie, R. Yu, Y. Zhang, and C. Yuen, "An efficient MAC protocol with selective grouping and cooperative sensing in cognitive radio networks," *IEEE Trans. Veh. Technol.*, vol. 62, no. 8, pp. 3928–3941, Oct. 2013.
- [28] H. Hu, H. Zhang, and Y.-C. Liang, "On the spectrum- and energy-efficiency tradeoff in cognitive radio networks," *IEEE Trans. Commun.*, vol. 64, no. 2, pp. 490–501, Feb. 2016.
- [29] J. Wang, P. Urriza, Y. Han, and D. Cabric, "Weighted centroid localization algorithm: Theoretical analysis and distributed implementation," *IEEE Trans. Wireless Commun.*, vol. 10, no. 10, pp. 3403–3413, Oct. 2011.
- [30] Q. Chen, Y.-C. Liang, M. Motani, and W.-C. Wong, "A two-level MAC protocol strategy for opportunistic spectrum access in cognitive radio networks," *IEEE Trans. Veh. Technol.*, vol. 60, no. 5, pp. 2164–2180, Jun. 2011.
- [31] S. Pandit and G. Singh, "Backoff algorithm in cognitive radio MAC protocol for throughput enhancement," *IEEE Trans. Veh. Technol.*, vol. 64, no. 5, pp. 1991–2000, May 2014.
- [32] S.-S. Tan, J. Zeidler, and B. Rao, "Opportunistic channel-aware spectrum access for cognitive radio networks with interleaved transmission and sensing," *IEEE Trans. Wireless Commun.*, vol. 12, no. 5, pp. 2376–2388, May 2013.
- [33] S.-C. Lin and K.-C. Chen, "Spectrum-map-empowered opportunistic routing for cognitive radio ad hoc networks," *IEEE Trans. Veh. Technol.*, vol. 63, no. 6, pp. 2848–2861, Jul. 2011.
- [34] W. Li, J. Lei, T. Wang, C. Xiong, and J. Wei, "Dynamic optimization for resource allocation in relay-aided OFDMA systems under multiservice," *IEEE Trans. Veh. Technol.*, vol. 65, no. 3, pp. 1303–1313, Mar. 2016.
- [35] C. Stevenson, C. Corderio, E. Sofer, and G. Chouinard, *Functional Requirements for the 802.22 WRAN Standard*, IEEE Standard 802.22-05/0007r46, Sep. 2005.
- [36] M. Clerc and J. Kennedy, "The particle swarm—Explosion, stability, and convergence in a multidimensional complex space," *IEEE Trans. Evol. Comput.*, vol. 6, no. 1, pp. 58–73, Feb. 2002.
- [37] A. Ratnaweera, S. K. Halgamuge, and H. C. Watson, "Self-organizing hierarchical particle swarm optimizer with time-varying acceleration coefficients," *IEEE Trans. Evol. Comput.*, vol. 8, no. 3, pp. 240–255, Jun. 2004.



Shaojie Zhang received the M.Sc. and Ph.D. degrees in information and communication engineering from the National University of Defense Technology, Changsha, China, in 2012 and 2016, respectively. He is currently a Lecturer with the Army Aviation Institute of PLA and serves with the Academy of Military Sciences of PLA, Beijing, China. His research interests include cognitive radio networks and performance analysis and optimization.

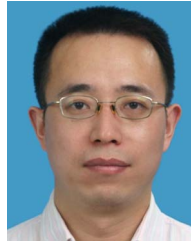


Abdelhakim Senhaji Hafid was a Senior Research Scientist with Telcordia Technologies (formerly Bell Communications Research), NJ, USA, researching on major research projects on the management of next generation networks including wireless and optical networks. He is a Full Professor with the University of Montreal, where he founded the Network Research Lab in 2005. He is also a Research Fellow with Interuniversity Research Center on Enterprise Networks, Logistics and Transportation. He supervised to graduation over 30 graduate students. He published over 200 journal and conference papers; he also holds three U.S. patents. He was also a Visiting Professor with the University of Evry, France, an Assistant Professor with Western University (WU), Canada, and a Research Director of Advance Communication Engineering Center (venture established by WU, Bell Canada, and Bay Networks), Canada, a Researcher with CRIM, Canada, and a Visiting Scientist with GMD-Fokus, Berlin, Germany. He has extensive academic and industrial research experience in the area of the management of next generation networks including wireless and optical networks, QoS management, distributed multimedia systems, and communication protocols.



Haitao Zhao (M'14) received the M.S. and Ph.D. degrees in information and communication engineering from National University of Defense Technology (NUDT), Changsha, China, in 2004 and 2009, respectively. He visited the Institute of Electronics, Communications, and Information Technology, Queen's University of Belfast, U.K. from 2008 to 2009 and conducted Post-Doctoral research with Hong Kong Baptist University from 2014 to 2015. He is currently an Associate Professor with the College of Electronic Science, NUDT. His

main research interests include cognitive radio networks, self-organized networks and cooperative communications. He is currently a member of ACM, World-Wide University Network Cognitive Communications Consortium, and also a Mentor Member for IEEE 1900.1 Standard. He has served as a TPC Member for IEEE ICC'14-17, Globecom'15-17 and a guest editor for several international journal special issues on cognitive radio networks.



Shan Wang is an Associated Professor with College of Electronic Science, National University of Defense Technology. His research interests include software communication architecture and wireless networks technologies, such as ad-hoc, VANETs, and cognitive networks.